Technical Report, IDE0801, January 2008

Identifying Deviating Systems with Unsupervised Learning

Master Thesis in
Computer Systems Engineering

Georg Panholzer

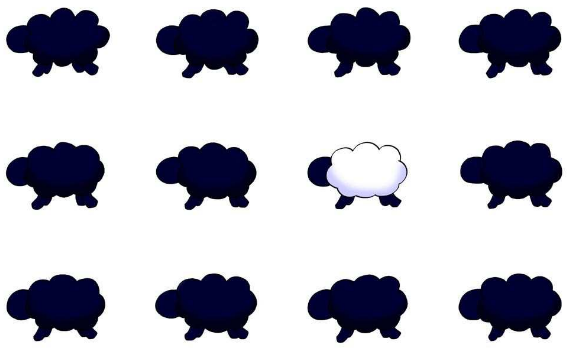

School of Information Science, Computer and Electrical Engineering
Halmstad University

Identifying Deviating Systems with Unsupervised Learning

School of Information Science, Computer and Electrical Engineering
Halmstad University
Box 823, S-301 18 Halmstad, Sweden

January 2008

Acknowledgement

Everything makes sense a bit at a time. But when you try to think of it all at once, it comes out wrong.
Terence David John Pratchett

First of all I want to thank my supervisor Prof. Thorsteinn Rögnvaldsson, whose advices and suggestions helped me during the whole time of preparing and writing this thesis.

I also want to thank my parents for providing me the possibility to study abroad.

Special thanks goes to Stephanie for all her love, patience and encouragement.

The cover illustration is generously provided by Sharon Rosa.

The motion capturing data set "CMU Database" was obtained from `http://mocap.cs.cmu.edu`. The database was created with funding from NSF EIA-0196217.

The motion capturing data set "MIT Data set" was obtained from `http://people.csail.mit.edu/ehsu/work/sig05stf`.

Details

First Name, Surname:	Georg Panholzer
University:	Halmstad University, Sweden
Degree Program:	Computer Systems Engineering
Title of Thesis:	Identifying Deviating Systems with Unsupervised Learning
Academic Supervisor:	Prof. Thorsteinn Rögnvaldsson

Abstract

We present a technique to identify deviating systems among a group of systems in a self-organized way. A *compressed representation* of each system is used to compute similarity measures, which are combined in an *affinity matrix* of all systems. *Deviation detection* and *clustering* is then used to identify deviating systems based on this affinity matrix.

The compressed representation is computed with *Principal Component Analysis* and *Kernel Principal Component Analysis*. The similarity measure between two compressed representations is based on the angle between the spaces spanned by the principal components, but other methods of calculating a similarity measure are suggested as well. The subsequent deviation detection is carried out by computing the probability of each system to be observed given all the other systems. Clustering of the systems is done with *hierarchical clustering* and *spectral clustering*.

The whole technique is demonstrated on four data sets of mechanical systems, two of a simulated cooling system and two of human gait. The results show its applicability on these mechanical systems.

Keywords

Deviation Detection, Clustering, Eigen-Subspace, Machine Learning

Contents

List of Figures

List of Tables

1 Introduction

Today's mechatronical systems like vehicles, robots or planes include a vast amount of embedded systems that are used to control and monitor their actions. About 100 micro processors and more than 2000 sensors are built into modern luxury-class cars. While some control safety-critical systems like breaks or airbags, others are essential to run the car, e.g. the engine control unit (ECU) which is responsible for fuel injection, spark time etc.

Each of these microprocessors logs its measurements and actions. This enables manufacturers and operators to collect exact data about the runtime behavior, which can then be used to find patterns (e.g. abnormalities after a certain sequence of events) that help to precisely identify faults and their sources. Precise findings facilitate to choose suitable counteractions and adapt service intervals, predict lifecycles and increase productivity.

On the other hand, a huge amount of data is produced. Generally this data is very complex and so specialized personnel and a lot of time is required to to have the data analyzed. Hence, automatic systems are needed to take over or ease this task.

Such systems have to follow certain constraints:

- A compressed representation of the raw data is essential to reduce the amount of data. This reduces transmission time which allows to use transmission techniques with low bandwidth (e.g. wireless transmission) and also results in a better scalability to a big number of systems.

- The system has to be able to detect deviations that have not occurred before, as it is (almost) impossible to think of all possible states beforehand. Thus, the system has to be self-organizing to adapt to the parameters of the monitored system automatically.

A lot of different forms of deviation detection methods have been used with a very wide variety of tasks either to clean data for further usage or detect faulty systems and behavior patterns. Depending on the author and field of application they are, for example, called deviation detection, outlier detection, novelty detection, anomaly detection, noise detection or exception mining. We will use the term *deviation detection*, as we feel that this most appropriately describes the process of finding systems that behave differently from a group of systems.

When used to clean data for further usage it is most often referred to as outlier detection. In machine learning and data analysis this is done to remove observations that are either *erroneous* (due to e.g. a faulty sensor) or normal measurements of a *rare condition* that is under-represented in the data set and difficult to derive an exact model for. Including observations of both cases generally results in a worse model of the actual data. Outlier detection and removal is often done by visual inspection of histograms, box plots or scatter plots. More sophisticated techniques include supervised classification, where data known to be normal or abnormal is pre-labeled. Classifiers are built upon these data and then used to classify the rest of the data.

Another application of deviation detection is to detect faulty systems or deviating behavior patterns. This is often a very important task as deviations could indicate faulty conditions which can lead to severe damage or even result in danger for users. Also it might point out fraudulent usage or decreased performance. Of course under any of those conditions it is beneficial to have a system that automatically detects deviating systems.

In either way most deviation detection systems are designed for a specific purpose.

1.1 Problem formulation

The goal of this thesis is to show that it is possible to detect “abnormal” systems in a group of systems without much prior knowledge about the systems. The proposed approach works offline, i.e. the whole data set is available before processing, but can be extended to an online version.

The approach is based on the assumption that “abnormal” systems deviate from “normal” systems if an appropriate representation is used. Deviating systems are those which do not behave like the bulk of systems. The challenges are to find such an appropriate representation in a self-organized way, compare these representation and then detect deviations.

The task is divided into three sub-tasks:

1. *How to represent an individual system?*

   This step extracts features that are “important”, i.e. those components that describe the systems behavior. The outcome of this step is a more efficient representation, which has to cover the relevant part of the total variance in the data while being as compact as possible.

2. *How to compare groups of systems?*

   This step provides the ability to compare the representation of systems with each other. Therefore, a suitable metric has to be defined. Based on this metric, a so-called *affinity matrix* for a group of systems is computed that contains a similarity measure for each pair of systems.

3. *How to detect deviating systems from the norm?*

   The deviation detection in this step is done in two different ways.

   One approach is to compute the probability for each system to be observed given all the other systems. In a “healthy” group where the majority of systems behave “normally”, the probability to observe an “abnormal” system should be very low.

> The other approach is based on clustering the group of systems. In this case, the “normal” systems should form one big cluster while the “abnormal” systems form one or more clusters with a small population.

Apart from the method proposed by Byttner et al. (2008), we are not aware of any approach that automatically tries to find a suitable compressed representation and at the same time detect deviating systems.

2 Background

Comprehensive summaries about the state of the art in deviation detection in a number of different domains can be found in Markou and Singh (2003a,b) and Hodge and Austin (2004).

Markou and Singh (2003a) present a survey of statistical approaches. These approaches are based on building a distribution model and then estimating the probability that a given observation belongs to this model. Such approaches mostly do not require assumptions on the nature of training data, but are dependent on their amount and quality. In general, statistical approaches are fast to compute and easy to explain and understand. In an successive paper, Markou and Singh (2003b) describe various neural network based outlier detection methods, but conclude that these have not been studied as detailed as statistical approaches and therefore guidelines on the applicability of certain approaches on a given data type are missing.

Hodge and Austin (2004) divide the field of outlier detection into three fundamental types: outlier detection without (much) prior knowledge (*unsupervised clustering*), model-based outlier detection with models for normality and abnormality (*supervised classification*) and model-based outlier detection with only a model for normality or(in very few cases) abnormality (*semi-supervised classification*). Further on, they describe statistical, as well as *artificial neural network* (ANN) approaches from all these types for different kinds of data sets and with different methodologies in order to provide an overview over the various techniques and their fields of application. They conclude that there is no generic approach and give advices on what to keep in mind when developing an outlier detection system. Generally, data preprocessing is a very important issue that can severely improve detection performance. Since data preprocessing is based on specific knowledge of the application, it requires an expert on the application and is often very time consuming. Additionally it results in a poor generalization to other application.

A highly active area of research is the field of *intrusion detection systems* (IDS). An IDS is used to detect malicious behavior patterns in computer systems and networks. Techniques for IDS range from simple, rule based approaches to systems which use *artificial immune systems* (AIS). AIS are inspired by the human immune system, which can detect and defend already known as well as previously unseen invaders. Aickelin et al. (2004) give a summary of AIS based IDS but conclude that these approaches are still in an early stage of development and have much room for improvements.

Lakhina et al. (2004) propose a *subspace method* for IDS, which uses *principal component analysis* (PCA) to compress the high dimensional set of network traffic measurement into two subspaces for normal and anomalous network conditions. Therefore, they compute the principal components and projections of the data. The separation into two subspaces it then done by examining the projection along each principal component. As son as a projection exceeds a certain threshold (3σ deviation from the mean), that principal component and all subsequent principal components are assigned to the "anomalous subspace", while all previous components span the "normal subspace."

Huang et al. (2006a,b) enhance this system into a framework for distributed network anomaly detection using the subspace method and demonstrate the applicability of PCA to compute a suitable compressed representation.

Vachkov (2006) uses the *Neural Gas* (NG) algorithm, an extension to the *Self-Organizing Map* (SOM), to compress the data collected on a hydraulic excavator. The compression is done by running the NG algorithm on 1200 observation to produce 60 nodes and than using these 60 nodes combined with their weight (i.e. the number of observations that support this node) and their width (i.e. the spread of the supporting observations) as a compressed representation of the excavators behavior. This automatically generated compressed representation is then transferred from the operating site to a maintenance center, where the fault diagnosis is done. However, this fault diagnosis is based on either visual inspection of 2 parameters at a time and comparison to normal working conditions or a similarity evaluation with a knowledge base.

As PCA is used on a wide variety of data sets to, methods to compare the outcome of PCA on different systems is needed. Krzanowski (1979) proposed a method to compare PCA results on the same variables of different groups of individuals. Therefore, an angle-based similarity measure is used.

During the last years, subspace methods have attracted a lot of attention in the field of human face recognition. To calculate the distance between face subspaces an angle-based distance measures is proposed by Wang et al. (2006), which is further analyzed by Sun and Cheng (2006).

Byttner et al. (2008) propose a self-organized fault detection scheme for vehicle fleets. A low-dimensional representation (i.e. a model) of a sub-system of a vehicle is created and transferred to a monitoring center, where it is compared to a group of vehicles. A simulated cooling system with and without leakage is used to test the approach. For the presented results, linear models with up to three parameters and a time lag of one of these parameters are used. Results show that vehicles with severe leakage level strongly deviate from vehicles without leakage, while minor leakage level cannot be detected.

Several approaches show that compressed representations based on PCA are usable for deviation detection. Also, PCA is fast to compute and methods to compare PCA subspaces are available. Therefore, PCA will be used to compute system representations.

Since PCA can only find linear correlations among the systems variables, the nonlinear generalization Kernel PCA will be used as well.

An angle-based similarity measure to compare representations of numerous systems will be used.

The final deviation detection will be carried out with a simple statistical approach, as this is fast to compute and does not require any additional human intervention.

3 Methods

As outlined in Sec. 1.1, there are three distinct sub-tasks: system representation, comparison of representations, and deviation detection.

3.1 System representation

The representation of systems is an essential part of an application that has to work with a big amount of high dimensional data. The idea is to capture the dynamics of a system and the correlations among the variables that show the deviations while reducing the amount of data by transforming it to a more compact representation.

Such a representation can be a number of selected features from the original space, extracted features in a lower dimensional space or functions that describe the relationships of the data. Also forms where several observations are concentrated and represented by fewer proxies are possible.

A compact representation is generally desirable, since it reduces memory consumption and computation time. As we want to transmit the representation from the system that captured the data to a monitoring facility a compact form also lowers transmission time. This is crucial in environments where only low bandwidth or short time is available, e.g. radio transmission from a truck whenever it passes a monitoring station.

On the other hand the transformation to a compact representation is lossy, i.e. information from the original data is irretrievably lost.

It is therefore important to find a suitable representation that reduces the amount of data while it still captures enough of the information.

3.1.1 Feature Extraction

Feature extraction is a form of dimensionality reduction, which utilizes the facts that

- variables in the high dimensional space are often not independent, but rather influence each other in various ways
- data is not spread over the whole high dimensional space, but may lie in a small region

to extract a small number of features that are "important" to describe the underlying phenomenon.

Common feature extraction techniques include linear and nonlinear forms of principal component analysis, *independent component analysis*, *canonical correlation analysis* and *latent semantic analysis*.

Besides these techniques, clustering methods can be used to group the raw data and then extract features from the resulting clusters. For example, Vachkov (2006) trains a SOM with the collected raw data and uses the resulting nodes as features.

The two techniques used in this work are PCA and Kernel PCA. Both are described in the following sections.

3.1.2 Principal Components Analysis

PCA is a well known technique which is easy to implement and fast to compute. Lakhina et al. (2004) show that PCA features are useful to detect deviations in computer networks.

Principal components analysis (PCA, also known as *Karhunen-Loève-Transfrom* or *proper orthogonal decomposition*) is based on the assumption that some variables are linearly correlated and thus can be recoded using a fewer number of linearly uncorrelated features.

PCA is a linear transformation that transforms a data set to a new orthogonal coordinate system, where the first axis is the direction of the greatest variance (the first principal component), the second axis is the direction of the second greatest variance (the second principal component) and so on.

In most cases dimensionality reduction with PCA is done by using only the first few principal components such that e.g. 95% of the total variance (i.e. the total spread of the data) is captured, since it is often assumed that the relevant information in the data is also adding the most variance.

In contrast to this, Lakhina et al. (2004) use minor components to detect anomalies in network traffic.

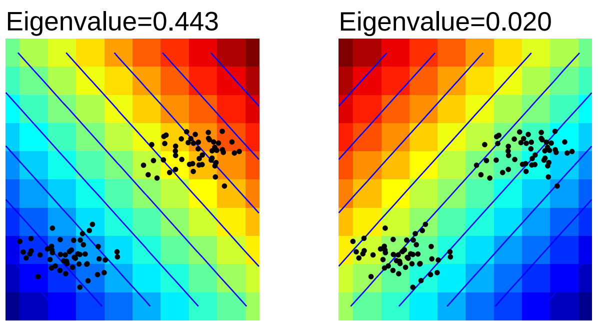

Figure 3.1: Example of PCA on a synthetic data set; the blue contour lines are perpendicular to the principal components and along these lines the principal components value is constant.

3.1.2.1 Calculation of the Principal Components

Suppose a vector $\mathbf{x}$ of m d-dimensional observations $\mathbf{x}_m, m = 1, \ldots, M$ that are centered so that $\sum_{m=1}^{M} \mathbf{x}_m = 0$. The covariance matrix for these observations is then

$$\mathbf{C} = \frac{1}{M} \sum_{m=1}^{M} \mathbf{x}_m \mathbf{x}_m^{\mathrm{T}}. \tag{3.1}$$

The principal components are the eigenvectors $\mathbf{V} = \mathbf{v_1}, \ldots, \mathbf{v_d} \in \mathbb{R}^d$ of $\mathbf{C}$ sorted by their eigenvalues λ and can be found by solving the eigenvalue equation

$$\mathbf{CV} = \lambda \mathbf{V}. \tag{3.2}$$

The observations are then projected onto these eigenvectors

$$\mathbf{x}' = \mathbf{xV}. \tag{3.3}$$

3.1.3 Kernel Principal Components Analysis

Kernel PCA is a generalization of PCA, which does not aim at finding principal components in the input space, but rather principal components of features that are non-linearly related to the variables in the input space. For example, this can be high order correlations of input variables.

The idea of kernel PCA is to perform a linear PCA in a space which is constructed by a nonlinear transformation of the input space. This transformation can easily be done by using a nonlinear kernel that maps from the input space to a higher dimensional space while allowing all calculations to be done in the input space. As shown in Schölkopf et al. (1998) kernel PCA extracts features that lead to better classification performance than linear PCA on a number of experiments.

The main drawback of Kernel PCA compared to normal PCA is that there is no method to reconstruct features in the input space from their kernel PCA mapping.

3.1.3.1 The Kernel Trick

The kernel trick is a method that provides the ability of using a non-linear algorithm to solve a non-linear problem. This works by utilizing Mercer's Theorem: any positive semi-definite , continuous and symmetric Kernel function $K(x, y)$ can be expressed by a dot product in a high-dimensional space. A kernel is positive semi-definite if $K(x, x) \geq 0$ for any x and symmetric if $K(x, y) = K(y, x)$.

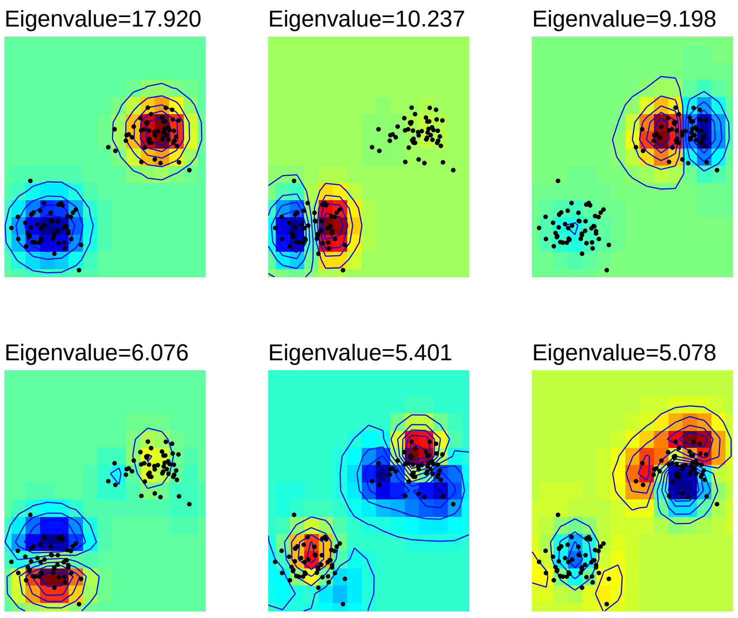

Figure 3.2: Example of kernel PCA with a Gaussian kernel on a synthetic data set; The contour lines are lines where the principal components value is constant, in the linear case these lines are perpendicular to the principal components.

The map

$$\Phi : \mathcal{X} \rightarrow \mathcal{H}, x \mapsto \Phi(x) \tag{3.4}$$

is called a feature map from the original space $\mathcal{X}$ into the feature space $\mathcal{H}$. Every dot product in this feature space can now be calculated as

$$\langle \Phi(x), \Phi(y) \rangle = K(x, y). \tag{3.5}$$

This means that the feature space $\mathcal{H}$ need not be known since all the calculations are done in the original space.

Commonly used kernels are:

$$\text{Polynomial:} \quad K(x, y) = \langle x, y \rangle^d \tag{3.6}$$

$$\text{Gaussian:} \quad K(x, y) = \mathbf{exp}(-\frac{||x - y||^2}{2\sigma^2}) \tag{3.7}$$

Further on, kernel PCA refers to kernel PCA with a Gaussian kernel.

Using this method, every linear technique that is solely based on dot products can be applied to non-linear problems.

3.1.3.2 Calculation of the Kernel Principal Components

Corresponding to PCA, suppose a vector $\mathbf{x}$ of m d-dimensional observations $\mathbf{x}_m, m = 1, \ldots, M$. The covariance matrix in the feature space $\mathcal{H}$ is calculated as

$$\overline{C} = \frac{1}{M} \sum_{m=1}^{M} \Phi(\mathbf{x}_m)\Phi(\mathbf{x}_m)^{\mathrm{T}}, \tag{3.8}$$

which leads to

$$(\Phi(\mathbf{x}_l) \cdot \overline{C}\mathbf{V}) = \lambda(\Phi(\mathbf{x}_l) \cdot \mathbf{V}) \tag{3.9}$$

for all $l = 1, \ldots, M$. There exists $\boldsymbol{\alpha} = \alpha_i, \ldots, \alpha_M$ such that

$$\mathbf{V} = \sum_{i=1}^{M} \alpha_i \Phi(\mathbf{x}_i) \tag{3.10}$$

Combining (Eq. 3.9) and (Eq. 3.10), we get

$$\frac{1}{M} \sum_{i=1}^{M} \alpha_i (\Phi(\mathbf{x}_l) \cdot \sum_{j=1}^{M} \Phi(\mathbf{x}_j))(\Phi(\mathbf{x}_j) \cdot \Phi(\mathbf{x}_i)) = \lambda \sum_{i=1}^{M} \alpha_i (\Phi(\mathbf{x}_l) \cdot \Phi(\mathbf{x}_i)) \tag{3.11}$$

By defining the dot product matrix $\mathbf{K}$ corresponding to kernel K as

$$\mathbf{K}_{ij} = (\Phi(\mathbf{x}_i) \cdot \Phi(\mathbf{x}_j)) \tag{3.12}$$

(Eq. 3.11) can be rewritten to

$$\mathbf{K}\boldsymbol{\alpha} = M\lambda\boldsymbol{\alpha}. \tag{3.13}$$

This eigenvalue problem is solved by diagonalizing $\mathbf{K}$ and the eigenvectors expansion coefficients α^n are normalized to

$$\lambda(\alpha^n \cdot \alpha^n) = 1. \tag{3.14}$$

Finally, to extract principal components corresponding to kernel K of point $\mathbf{x}$ the projections onto the eigenvectors are computed by

$$(K\mathrm{PC})_n(\mathbf{x}) = (\mathbf{V}^n \cdot \Phi(\mathbf{x})) = \sum_{i=1}^{M} \alpha_i^n (\Phi(\mathbf{x}_i) \cdot \Phi(\mathbf{x})). \tag{3.15}$$

3.1.4 Other nonlinear PCA methods

Hebbian Networks

By utilizing *Oja's Rule* which was introduced by Oja (1982), *artificial neural networks* (ANN) are able to compute principal components. When nonlinear activation functions are used, nonlinear principal components are found.

These methods have advantages when the input data are not stationary, but lack a geometric interpretation.

Deep Autoencoder

The deep autoencoder is a nonlinear generalization of PCA which uses an ANN with a bottleneck. It is trained by using the input x as desired output y. As these networks are big (typically with several hundred to thousand nodes and 5 to 11 fully connected layers) it takes a long time to train.

Hinton and Salakhutdinov (2006) show that the deep autoencoder significantly outperformed PCA on the reconstruction error on a number of data sets.

In contrast to PCA and kernel PCA, these methods do not compute new bases, but instead train ANNs. Comparing ANNs cannot be done with the methods to compare bases and was beyond the scope of this work.

3.2 System comparison

The features extracted in the system representation step have to be compared to be usable for deviation detection and clustering. In the case of PCA and Kernel PCA these features are principal components, which span an orthogonal space. As not all of the principal components are used, this space is further on referred to as subspace.

We thought about three methods to compare two subspaces: the angle between them, the overlapping volume and the reconstruction error of the data with interchanged subspaces.

The angle between two subspaces can be calculated as proposed by Krzanowski (1979). The measure of similarity is the sum of the squared cosines of the angles between all the eigenvectors. This measure is in the range of 0 (for non-overlapping spaces) to 1 (for coincident spaces) and symmetric, i.e. the similarity between the two subspaces A and B is equal to the similarity between B and A.

The overlapping volume between two subspaces can be based on hyper-cuboid where the side length are equal to the eigenvalues. This measure has the advantage of also taking the eigenvalues into account. It is symmetric, but is not limited to a range of 0 to 1.

A similarity measure based on the reconstruction error with interchanged subspaces can be calculated as follows: The principal components PC_A and PC_B are computed for the two systems A and B respectively. The data of system A are transformed to the new space span by PC_A and the reconstruction error E_{AA}^N when using only the first N principal components is calculated. Then the reconstruction error E_{AB}^N of transforming the data of system A to the space span by first N principal components of PC_B is calculated. This similarity measure is neither symmetric, nor in the range of 0 to 1.

As the properties of the angle-based similarity measure are very convenient when comparing different similarities, this measure is used further on. The successive methods rely on these properties and thus, to use any of the other methods, each similarity measure has to be rescaled to be in the range of 0 to 1. This, however, has to be done in a way that the relationships between similarity measures of different systems are represented correctly, i.e. pairs of systems with a similarity close to 1 are in fact more similar than pairs with a lower similarity measure.

3.2.1 Calculation of the Angle between two Subspaces

Suppose two subspaces L and M with N principal components. The matrices $\mathbf{L} = (l_1, \ldots, l_n)$ and $\mathbf{M} = (m_1, \ldots, m_n)$ contain these principal components as column vectors.

The angle θ_{11} between their first principal components is calculated as

$$\theta_{11} = arccos\sqrt{\langle l_1, m_1 \rangle}. \tag{3.16}$$

of the two vectors l_1 and m_1. A measure of similarity can be defined as

$$s_{11} = cos^2\theta_{11} = \langle l_1, m_1 \rangle. \tag{3.17}$$

As shown by Krzanowski (1979), this can be generalized to more than one principal component as

$$S(L, M) = \frac{1}{N}\sum_{i=1}^{N}\sum_{j=1}^{N} cos^2\theta_{ij} = \frac{1}{N}\mathbf{tr}\ \mathbf{L}^{\mathrm{T}}\mathbf{M}\mathbf{M}^{\mathrm{T}}\mathbf{L}. \tag{3.18}$$

This similarity measure lies between 0 for non-overlapping spaces and 1 for coincident spaces.

Wang et al. (2006) propose a *subspace distance* (SSD)

$$d_{wwf}(L, M) = \sqrt{N - \sum_{i=1}^{N}\sum_{j=1}^{N}(l_i^T m_j)^2}. \tag{3.19}$$

Sun and Cheng (2006) show that $d_{wwf}(L, M)$ is a proper distance measure, i.e. it satisfies the following properties:

- Non-negativity: $0 \leq d_{wwf}(L, M)$ for any L and M
- Symmetry: $d_{wwf}(L, M) = d_{wwf}(M, L)$
- Triangular inequality: $d_{wwf}(L, M) \leq d_{wwf}(L, \Gamma) + d_{wwf}(\Gamma, M)$

$d^2_{wwf}(L, M)$ is proportional to $S(L, M)$.

3.2.2 The Affinity Matrix

For more than two systems, the similarity measures (Eq. 3.18) between all subspaces were combined into an *affinity matrix* A. For k systems with their d-dimensional subspaces $X_1, ..., X_k$, this affinity matrix is

$$A = \begin{pmatrix} a_{11} & a_{21} & \cdots & a_{k1} \\ a_{12} & a_{22} & \cdots & a_{k2} \\ \vdots & \vdots & \ddots & \vdots \\ a_{1k} & a_{2k} & \dots & a_{kk} \end{pmatrix} \tag{3.20}$$

where

$$a_{i,j} = S(X_i, X_j). \tag{3.21}$$

This matrix is symmetric and the diagonal elements are 1.

Although we only use the angle based measure of similarity it is worth mentioning that the affinity matrix can as well be based on any other similarity measure, as long as the above mentioned properties apply.

The subsequent deviation detection and clustering methods are solely based on the affinity matrix and, consequently, it effectively decouples them from the feature extraction methods.

3.3 Deviation detection

The deviation detection is based on building a statistical model D of the affinities and from this compute the probability of each observation given D.

We assume that the affinities from a given observation of a data set to all the other observations follow a normal distribution. Although the affinity is limited (between 0 and 1) while the normal distribution extends to infinity, a small variance of the affinities results in a narrow probability distribution function, where the significant part lies between 0 and 1. For a reasonable data set this should hold. Otherwise either the system representation step failed to produce a suitable representation, i.e. a representation that preserves the relations between systems, or the systems are not similar at all.

The calculation of the probability to observe sample x given the data set S is done on both, the mean affinities and on the separate affinities.

Calculation of $P(x|S)$ based on the mean affinities:

1. Compute the affinity matrix A for $\{S, x\}$ (i.e. the set of all samples from S and the test sample x)
2. Compute the mean affinity $\overline{a}$ for every system in S, i.e. remove the diagonal and then take the mean of every column
3. Let $D \sim N(\mu_{\overline{a}}, \sigma^2_{\overline{a}})$, where $\mu_{\overline{a}}$ is the meanand $\sigma^2_{\overline{a}}$ is the variance of all $\overline{a}$
4. Calculate $P(x|S)$ as the cumulative distribution function of D at $\overline{a}_x$

Calculation of $P(x|S)$ based on the separate affinities:

1. Compute the affinity matrix A for $\{S, x\}$
2. For each system n of the N systems:
   - 2.1. Take the affinities of all other systems to system n and store them in a_n
   - 2.2. Let $D_n \sim N(\mu_{an}, \sigma^2_{an})$
   - 2.3. Calculate $P_n = P(x|S)$ as the cumulative distribution function of D_n at a_{xn}
3. Calculate $P(x|S)$ as the geometric mean $\sqrt[N]{\prod_{n=1}^{N} P_n}$

Both ways of calculating the probability $P(x|S)$ use the means and variances of the affinities. The mean and variance are sensitive to outliers. This shortcoming can be overcome by using a technique to derive a robust estimate of $P(x|S)$. One such technique is *bootstrapping*.

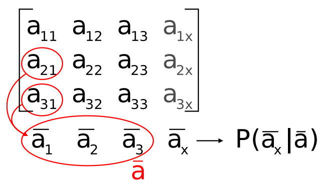
a_{11} a_{12} a_{13} a_{1x}
a_{21} a_{22} a_{23} a_{2x}
a_{31} a_{32} a_{33} a_{3x}
$\overline{a}_1$ $\overline{a}_2$ $\overline{a}_3$ $\overline{a}_x \longrightarrow P(\overline{a}_x|\overline{a})$
$\overline{a}$

(a) Mean affinities

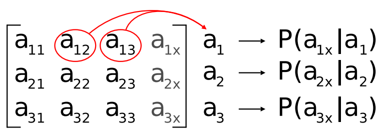
a_{11} a_{12} a_{13} a_{1x} $a_1 \longrightarrow P(a_{1x}|a_1)$
a_{21} a_{22} a_{23} a_{2x} $a_2 \longrightarrow P(a_{2x}|a_2)$
a_{31} a_{32} a_{33} a_{3x} $a_3 \longrightarrow P(a_{3x}|a_3)$

(b) Seperate affinities

Figure 3.3: The calculation of $P(x|S)$ on the mean affinities and on the separate affinities

3.3.1 Bootstrapping

Bootstrapping is a statistical resampling method introduced by Efron (1979). By random sampling with replacement it derives robust estimates of properties like mean or median of the underlying distribution.

The bootstrapping algorithm to compute the probability of observing a system x given data set S is as follows:

1. Take the set of measurements S of the size N and the system to test x.
2. Repeat M times
   - 2.1. Pick a random bootstrap sample BS from S. The size n of this sample is $0 < n < N$
   - 2.2. Compute the probability model for BS
   - 2.3. Compute $P_n(x|BS)$
3. Estimate $P(x|S)$ as the median of the set $\{P_1(x|BS), \ldots, P_N(x|BS)\}$

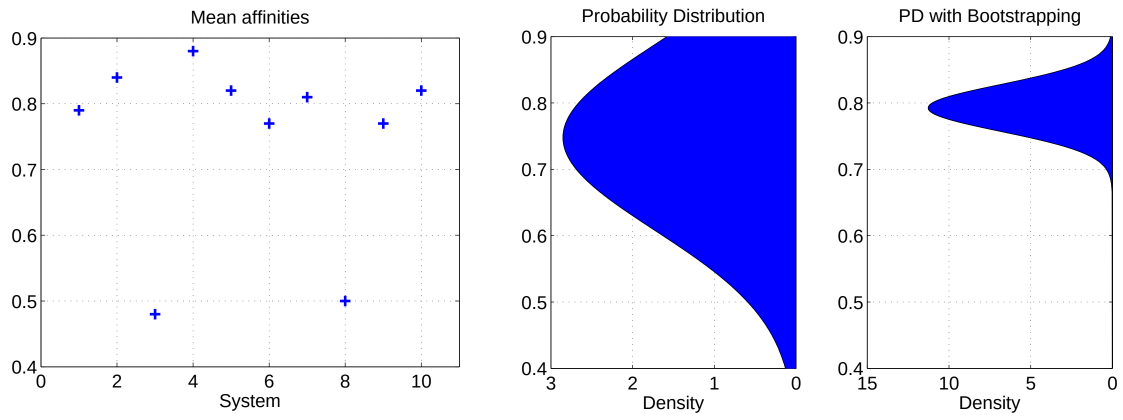

(a) Mean affinities **(b)** PD **(c)** PD with BS

Figure 3.4: The effect of bootstrapping on a synthetic data set with 20% outliers. (a) The mean affinities of a synthetic data set; (b) the probability distribution for the whole dataset; (c) the probability distribution with bootstrapping ($M = 20, n = 0.5$)

3.4 Clustering

The goal of clustering is to group a data set into a number of groups, such that the observations within one group are more similar to each other than to observations in other groups. The similarity between objects is calculated with a defined distance measure. Common distance measures are Euclidean distance or Mahalanobis distance, but also other measures can be used.

Clustering methods can be divided into two types: hierarchical and partitional clustering. Hierarchical clustering methods produce the clusters of each level based on the clusters of the previous level, while partitional clustering finds all clusters at once.

3.4.1 Spectral Clustering

Spectral clustering is a partitional clustering method. The idea of spectral clustering is based on concepts from spectral graph theory, which studies the properties of graphs with respect to the spectrum (i.e. the eigenvectors and eigenvalues) of its adjacency and Laplacian matrix.

In graph theory the grouping of a graph into two disjoint sets is done by simply removing the edges that connect the two sets and is called *cut*. The *size* of the cut is the sum of the weights of all removed edges. Minimizing this cut value leads to the optimal partition into two groups.

Shi and Malik (2000) introduce the *normalized cut* criterion to segment images and show how this can be done by solving a eigenvalue system. This method uses an affinity matrix that describes the similarity between any pair of nodes in the graph. In our case, this affinity matrix is calculated as described in Sec. 3.2.2.

To segment the graph, the eigenvalue system has to be solved. Clustering into k groups is then done by using k-means clustering on the eigenvectors.

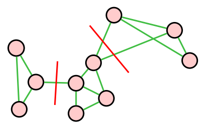

Figure 3.5: Example of Spectral Clustering, the red lines show the cuts

3.4.2 Hierarchical Clustering

Hierarchical clustering builds up or breaks down a hierarchy of clusters. Building up a hierarchy is called *agglomerative* hierarchical clustering, while breaking down is called *divisive* hierarchical clustering.

Agglomerative clustering starts at the lowest level, where each cluster contains only a single observation, and recursively reduces the number of clusters by merging the two closest ones (bottom-up). Divisive clustering starts with one cluster that covers the whole data set and recursively splits one cluster into two new clusters (top-down), where the split is chosen in a way that the two new clusters have the largest possible dissimilarity.

Hastie et al. (2001) state that divisive methods have potential advantages when aiming to partition the data set into a *small* number of clusters.

Often the splitting is done by applying k-means or k-medoids clustering with $K = 2$, but then of course such an approach depends on the starting configuration. An approach that avoids this was invented by Macnaughton-Smith et al. (1964). It starts with a single cluster G. The observation whose average dissimilarity to all other observations is largest is removed from G and forms a new cluster H. At the next step the observation with the largest average dissimilarity from H minus the average dissimilarity from G is transferred to H. This is done until the largest value becomes negative, which means that there are no more observations in G that are (on average) closer to H. This process is visualized in Fig. 3.6.

Clustering into more than two clusters is done by recursively applying hierarchical clustering on the resulting clusters.

This method is solely based on the measure of similarity and does not depend on any (random) starting configuration.

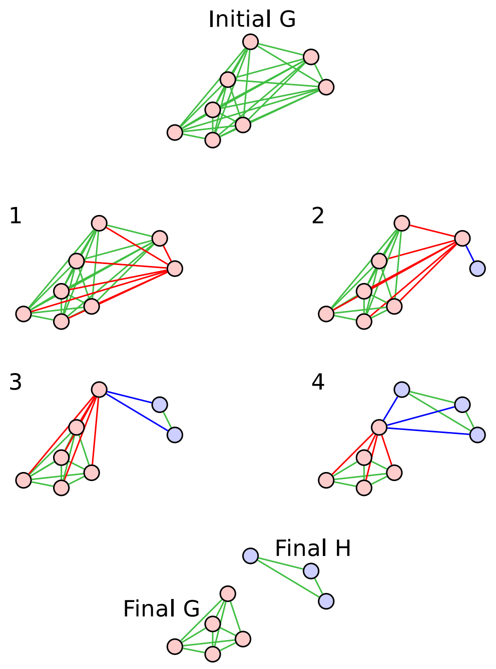

Figure 3.6: Hierarchical clustering with the Macnaughton-Smith approach of cluster G into clusters G and H. The red systems belong to cluster G and the blue ones to H.

4 Data sets

We wanted to test our approach on two different types of mechatronical systems. Hence we used

- data of a simulated vehicle cooling system
- human gait data.

The cooling system data is also analyzed in Byttner et al. (2008).

We use the human gait pattern to illustrate a possible humanoid robot.

4.1 Vehicle Cooling System

The cooling system data is provided by a vehicle manufacturer and is generated with a simulation model of a cooling system.

Every simulation has at least 1600 consecutive observations with 51 signals such as fan speed, cooling water and oil temperature, engine speed and other parameters that are considered relevant for the cooling system.

Two data sets that simulate different failures are available. Both sets contain a number of reference systems without any failure and systems with failures at different severity levels. The systems are from one of three different weight classes (15 tons, 18 tons and 23 tons) and three different ambient temperatures (10°C, 20°C and 30°C).

4.1.1 Healthy Systems

The leakage data set contains 9 healthy systems, one from each weight class and ambient temperature. These systems are denoted by their weight and temperature, e.g. *15t10*.

The data set of the soiled model contains another three healthy systems for each weight class at a constant ambient temperature of 20°C. Further on, these systems are denoted by the suffix *_s0* e.g. *15t20_s0*.

Together, these 12 systems form the "normal" data set.

4.1.2 Systems with a Leakage

This data set was generated with a model that simulates a leakage in the cooling system. The model has a certain amount of air added to the coolant mixture, which lowers its heat capacity.

There are three different severity levels, 20%, 40% and 60% air for each of the weight class and ambient temperature, making a total of 27 leakage systems.

Systems with a leakage are labeled with a suffix like *_l20*.

4.1.3 Soiled Systems

The model used for this data set simulates a cooling system with a soiled radiator. A given fraction of the radiators surface is covered with dirt, lowering its ability to emit heat and therewith the cooling efficiency.

Again, there are three different levels of severity, 15%, 30% and 50% of the surface for each of the three weight classes at an ambient temperature of 20°C.

Soiled systems are denoted with a suffix like *_s15*.

4.2 Human Gait Data

Two different motion capturing data sets were used. Unfortunately their formats are incompatible and therefore they had to be examined separately.

4.2.1 CMU Data Set

This data set was obtained from the CMU Graphics Lab Motion Capture Database in *Acclaim Motion Capture* (AMC) format. These files contain 62 features that are captured at a frame rate of 120 frames per second.

12 samples for "normal" walking and one "faulty", limping samples from five different subjects were picked. After visual inspection they were trimmed to 300 frames and the toe and hand features[1] and the absolute position in the world frame were removed. Tab. 4.1 shows the used subjects and trials.

Style	Subject	Trial
"normal" walking	5	1
	6	1
	7	1, 2, 3, 4, 6
	8	2, 3, 4, 7, 11
limping	17	5

Table 4.1: CMU Data Set subjects and trials

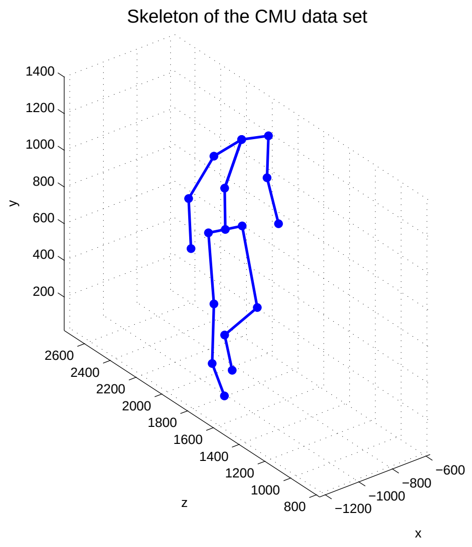

Figure 4.1: Example skeleton of the CMU data set

[1]CMU Graphics Lab states that these features tend to be noisy and visual inspection confirmed this.

4.2.2 MIT Data Set

The MIT data set was used by Hsu et al. (2005). It contains various different walking styles: normal walking, jogging, waddling, swaying, walking sideways and limping. Three different speeds are available for each style, slow, medium and fast that vary in step size.

The format used for these data does not divide the information into a skeleton that defines the connections and distances between joins and the motion data that states the angles for each joint at a time. Instead it gives angles and distance in x, y and z direction with respect to its parent joint. As the offsets are only dependent on the person, but not on the walking style, they were removed.

Visual inspection revealed that the sections featuring the specific walking style were interrupted by sections of normal walking. Hence, it was necessary to extract continuous sections of the specific walking style, which all show walking on a straight line and are 300 frames long.

Sample	Style	Speed
1 - 4	Normal	Slow
5 - 8	Normal	Medium
9 - 12	Normal	Fast
13	Jog	Slow
14	Jog	Medium
15	Waddle	Fast
16	Sway	Medium
17	SideRight	Slow
18	SideRight	Medium
19	SideRight	Fast
20	Limp	Slow
21	Limp	Medium
22	Limp	Fast

Table 4.2: MIT Data set subjects and trials

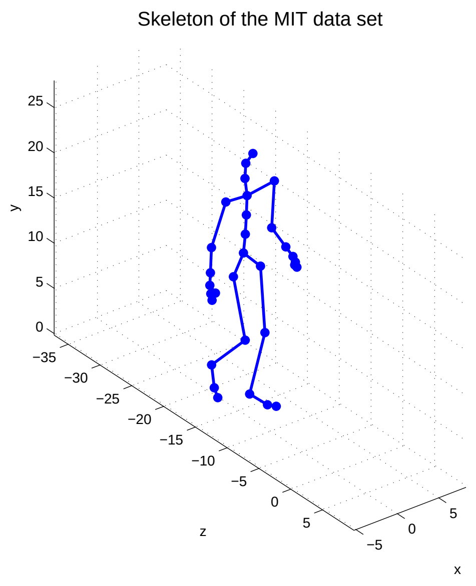

Figure 4.2: Example skeleton of the MIT data set

5

Results and Discussions

5.1 Deviation detection

This section presents the results of the deviation detection method on the four data sets. Observations that have a likelihood below 5% are considered as deviating.

Throughout this section the data sets are split into their naturally distinct parts of “normal” and “faulty” systems.

5.1.1 Cooling System with a Leakage

5.1.1.1 Deviation Detection based on PCA

Principal components analysis on the whole data set revealed that six principal components were sufficient to capture at least 95% of the data, i.e. the reconstruction error with 6 principal components was smaller than 5% for all systems. The reconstruction error with different numbers of principal components for system *15t20_s0* can be seen in Fig. 5.1.

At first, the normal set was investigated alone. Bootstrapping was used with a *leave one out* sampling. To verify the usability of the 95%-preservation approach, the number of principal components was varied from 2 to 11. The results of the bootstrapping are given in Tab. 5.1 and the details of the bootstrapping on the mean affinity with 6 principal components can be seen in Fig. 5.2.

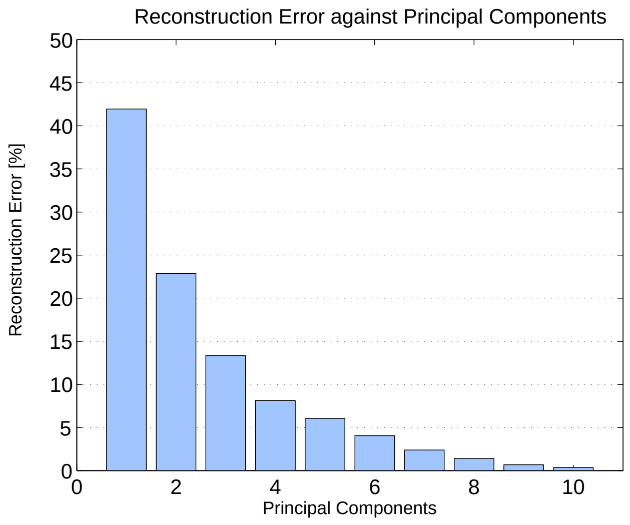

Figure 5.1: Reconstruction Error against Principal Components for System *15t20_s0*

Number of PC	Deviating Systems (mean affinity)	Deviating System (affinity)
2	No deviation	No deviation
3	15t30	No deviation
4	15t10	15t10
5	23t30	No deviation
6	**18t30**	**18t30**
7 - 11	18t30	18t30

Table 5.1: Results of bootstrapping on normal systems

The deviation detection was then carried out with bootstrapping on the mean affinity and on the separate affinities in a *one versus all* fashion, i.e. one "faulty" system was compared to all "normal" systems. Again the number of principal components was varied from 2 to 11 to evaluate their influence on the detection performance. Tab. 5.2 shows the number of detected deviations out of the 27 "faulty" systems.

Discussion

As Tab. 5.1 shows, with six and more principal components system *18t30* was consistently detected as deviating. It was, however, impossible to check if there were any errors in the simulation and system *18t30* was therefore not removed from the

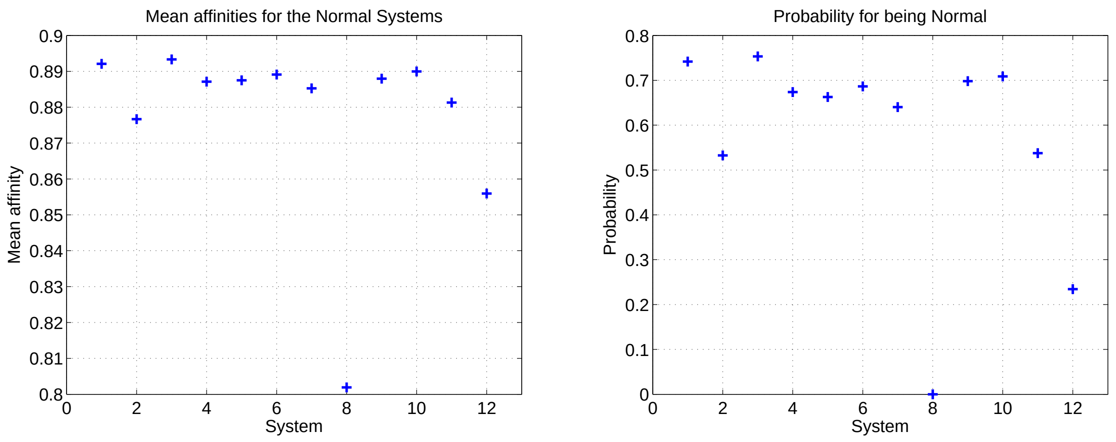

(a) Mean affinities (b) Probabilities

Figure 5.2: (a) The mean affinities within the group of normal systems (b) the probabilities calculated with bootstrapping and leave-one-out sampling on the mean affinities

Number of PC	Deviating Systems (mean affinity)	Deviating Systems (affinity)
2	5	5
3	13	14
4	8	8
5	19	3
6	**27**	**27**
7 - 11	27	27

Table 5.2: Number of systems detected as deviations out of 27 "faulty" leakage data samples

"normals".

Tab. 5.2 shows that with six and more principal components it was also possible to detect all 27 "faulty" systems as deviations from the "normal" set when the "normal" set includes system *18t30*.

These results clearly indicate that the approach works on this data set.

5.1.1.2 Detection Performance with Erroneous Normals

To evaluate the stability of the detection performance against "faulty" systems within the group of "normals", 0 - 4 random faulty systems were added to the set of normals. Deviation detection was then done 100 times and the detection performance was

Erroneous	Test	Detected Deviations			
Samples	Samples	Mean	Std.Dev	Min	Max
0	27	27	0	27	27
1	26	20.4	6.7	3	26
2	25	10.4	4.6	2	18
3	24	5.0	2.3	2	12
4	23	3.6	1.6	2	9

Table 5.3: Detection performance with erroneous samples in the "normals" set, bootstrapping on mean affinities with 6 principal components

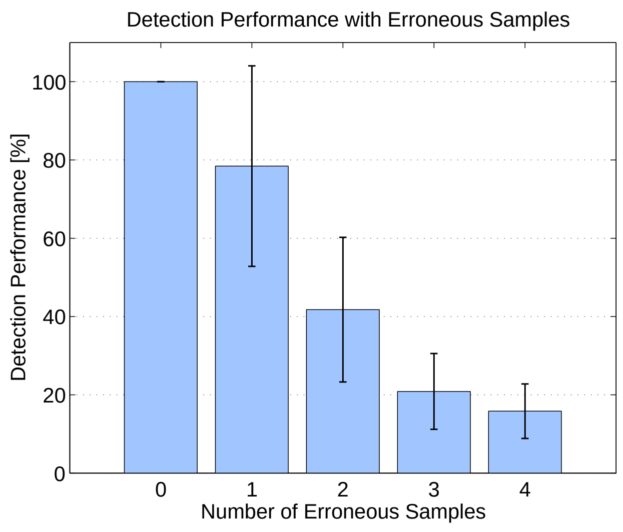

Figure 5.3: Detection rate with erroneous samples in the "normals" set, bootstrapping on mean affinities with 6 principal components

measured. The results for deviation detection using the mean affinity are given in Tab. 5.3 and Fig. 5.3 and those for deviation detection using the separate affinities are given in Tab. 5.4.

It is worth noting for this set of experiments the group of "normals" already contained a possibly "faulty" system, namely *18t30*.

Discussion

Assuming that system *18t30* is erroneous, the "normals" already contain 8% erroneous samples. By adding 4 more erroneous samples to this set, more than 30% of the

Erroneous	Test	Detected Deviations			
Samples	Samples	Mean	Std.Dev	Min	Max
0	27	27	0	27	27
1	26	18.1	4.1	2	24
2	25	4.4	1.7	1	8
3	24	2.1	0.4	1	5
4	23	1.8	0.6	0	5

Table 5.4: Detection performance with erroneous samples in the "normals" set, bootstrapping on separate affinities with 6 principal components

"normals" are faulty. It is comprehensible that a deviation detection does not perform well under this conditions.

5.1.1.3 Deviation Detection based on Kernel PCA

Using bootstrapping on the outcome of Kernel PCA feature extraction did not give usable results. Even though bootstrapping with mean affinities flagged some systems as outliers the detected systems varied and, thus, we assume that these detections are highly dependent on the random composition of the bootstrap sample.

This is caused by the fact that the affinities between systems of different weight classes are very low (i.e. they are very dissimilar, see Fig. 5.8 a in Sec. 5.2.1.3) and so for each system, more than $\frac{2}{3}$ of all the other systems are very dissimilar.

5.1.2 Soiled Cooling System

As described in Sec. 4, the "normal" systems for the soil data set were the same as for the leakage data set, while the "faulty" set was made up by 9 soiled systems instead of 27 systems with a leakage.

PCA revealed that six principal components were again sufficient for the "faulty" systems of this data set and thus the trials from the previous section were repeated.

Applying bootstrapping did not result in any stable detections when using fewer than six principal components. Three deviating systems were detected when using six or more

Number of PC	Deviating Systems (mean affinity)	Deviating Systems (affinity)
2	0	0
3	2	2
4 , 5	0	0
6	**3**	**3**
7 - 11	3	3

Table 5.5: Number of systems detected as deviations out of 9 “faulty” soil data samples

principal components. These three systems were *18t20_s50*, *23t20_s30* and *23t20_s50.*

Tab. 5.5 shows the number of detected deviations out of the 9 “faulty” systems.

Discussion

A soiled radiator does not effect the cooling system as severely as a leakage does. Consequently, it is understandable that a soiled system is harder to detect than a system with leakage. This is also reflected by the detection performance of this data set.

The three detected systems *18t20_s50*, *23t20_s30* and *23t20_s50* are those that one would most likely expect to be affected by soil in the cooling system, as these are the heavy ones with a high soil level.

5.1.3 Human Gait Data - CMU Data Set

This data set contained 12 trials of “normal” walking from four different subjects and one trial of limping from yet another subject. It required 13 principal components to describe 95% of the variance of the original data. As for the vehicle cooling system data sets, different numbers of principal components were tried out. In this case the number was varied from 8 to 18 (13 ± 5).

First of all, the whole data set was inspected with bootstrapping on the mean affinity as well as on the separate affinities. The results are in Tab. 5.6.

Number of PC	Deviating Systems (mean affinity)	Deviating Systems (affinity)
8	5/1, 17/5	8/4
9, 10	5/1, 17/5	No deviation
11	5/1, 17/5	17/5
12-18	17/5	17/5

Table 5.6: Results of bootstrapping on the CMU data set

Number of PC	Deviating Systems (mean affinity)	Deviating Systems (affinity)
8-10	1	0
10-18	1	1

Table 5.7: Detection Performance on the CMU data set

Subsequently a *one versus all* test was done too with both deviation detection methods. Tab. 5.7 shows that 8 principal components were sufficient to detect the limping individual with bootstrapping on the mean affinity. Bootstrapping on the separate affinities worked with 10 and more principal components.

Discussion

The inspection of the whole data set showed that bootstrapping on the mean affinity as well as on the separate affinities was able to detect the limping individual with 12 and more principal components. Obviously, the 8 features were already sufficient to describe the difference of trial *17/5* from the others but 12 features were necessary to cover the similarity of trial *5/1* to the others.

5.1.4 Human Gait Data - MIT Data Set

From the 54 features that were captured for the MIT data set PCA produced 10 which were sufficient for the 95% approach. However, 5 - 15 principal components were used for the experiments.

Number of PC	Deviating System (mean affinity)	Deviating System (affinity)
5 - 7	No deviation	No deviation
8, 9	Normal Slow 4	Normals Slow 4
10 - 12	No deviation	No deviation
13 - 15	Normal Slow 1	No deviation

Table 5.8: Results of bootstrapping on the 12 “normals” of the MIT data set

Number of PC	Deviating Systems (mean affinity)	Deviating Systems (affinity)
5-15	10	10

Table 5.9: Detection Performance

The inspection of the “normal” walking styles did not reveal any outstandingly deviating sample, although the samples *Slow 4* and *Slow 1* were detected as outliers with some numbers of principal components. Tab. 5.8 gives all results.

During the subsequent deviation detection, where one of the “other” samples was compared to the 12 “normals”, all 10 “others” were detected as deviating with any number of principal components, see Tab. 5.9. The affinity matrix shown in Fig. 5.4 illustrates the reason for this.

To have more variations in the systems that are considered “healthy”, the two jog samples were added to the normals. The deviation detection was then redone using this enlarged set of healthy systems as reference. The samples featuring waddling and swaying styles were not detected as deviations in this experiment, while most of the samples showing walking sideways and limping were detected. The detailed results are given by Tab. 5.10.

Discussion

The fact that none of the “normals” is detected as outlier is not very surprising as all the samples show the same individual and essentially only differ in walking speed.

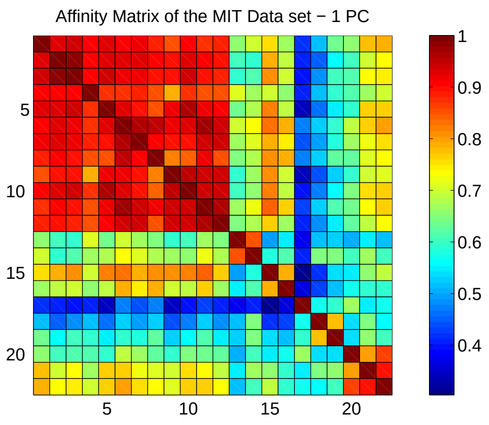

(a) Affinity matrix with 1 principal component

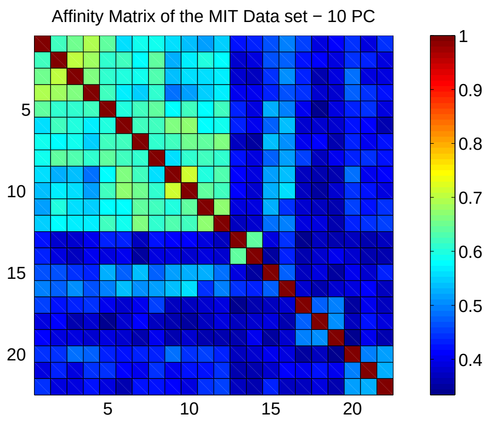

(b) Affinity matrix with 10 principal components

Figure 5.4: Affinity matrices of the MIT data set, 1 and 10 principal components

Number of PC	Deviating Systems (mean affinity)	Deviating Systems (affinity)
5 - 8	SideRight, Limp	SideRight, Limp
9	SideRight, Limp	SideRight, Limp Medium and Fast
10	SideRight, Limp	SideRight Medium and Fast, Limp Fast
11	SideRight, Limp	SideRight, Limp Medium
12	SideRight, Limp	SideRight, Limp Slow
13	SideRight, Limp	SideRight Medium and Fast, Limp Medium
14	SideRight, Limp Medium and Fast	SideRight
15	SideRight	SideRight

Table 5.10: Results of bootstrapping, Normals + Jog vs. Rest

The affinity matrices in Fig. 5.4 perfectly show the reason for the good results of the deviation detection. The affinities within the “normal” samples are very high compared to the other affinities.

The results of the enlarged set of healthy systems make perfect sense, as walking sideways is odder than limping. However, both are odder than jogging and therefore detected as deviations, while waddling and swaying are closer to normal.

5.2 Clustering

5.2.1 Cooling System with a Leakage

5.2.1.1 Spectral Clustering on PCA

Like the deviation detection, the clustering was based on the affinity matrix. The number of principal components used to calculate the affinity matrix was again determined with the 95% preservation approach. Fig. 5.5 a shows a graphical representation of the affinity matrix for the leakage data set.

Spectral clustering was done with the *normalized cut partitioning algorithm*, which uses the *k-means algorithm*. The cluster centers were initialized randomly, which influenced the outcome. The clustering was therefore repeated 100 times. The result was a matrix with the probabilities that systems were grouped together. Such matrices are shown in Fig. 5.6 a-c.

To find usable numbers of clusters the clustering was done for 2 - 10 clusters and the number of groupings $> 90\%$ was observed. Groupings $> 90\%$ indicated that the related systems were consistently grouped together and are not dependent on the random initialization. As the number of groupings varied, this experiment was repeated 15 times. Additionally the clustering was performed on random affinity matrices. These random affinity matrices were constructed such that they had the same properties as real affinity matrices, i.e. they were symmetric with ones on the diagonal. The result can be seen in Fig. 5.5 b.

Additionally, for every clustering the probability for each system to belong to the cluster where its assigned to and to belong to the other cluster(s) is calculated. This probability is calculated as the normal cumulative distribution function for the mean affinity of a certain system in the cluster given the cluster.

The detailed clustering was done for 2, 3 and 4 clusters. All the results are shown in Fig. 5.6.

Clustering into two clusters nicely separated the two groups of “normals” and “faulty” systems, except for the system *18t30*, which was clustered as “faulty”. The probability

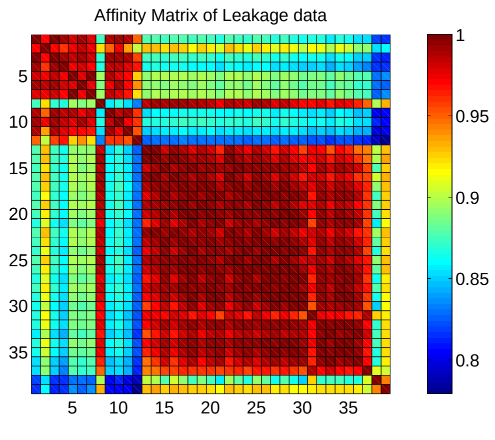

(a) Affinity Matrix

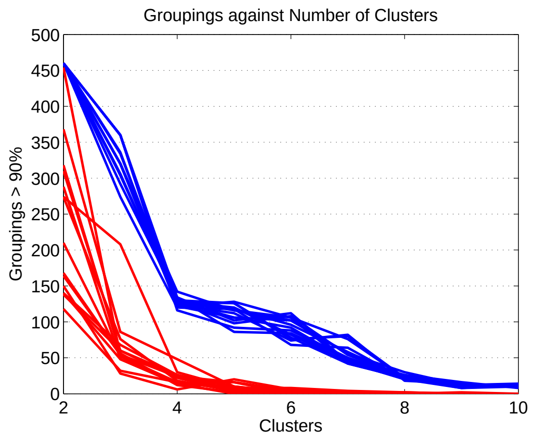

(b) Groupings against the number of clusters

Figure 5.5: (a) The affinity matrix of the Leakage data set (b) Number of systems grouped together in at least 90 out of 100 cases. Blue is for 15 spectral clusterings on the affinity matrix in (a), red is for 15 random affinity matrices

for any system of the "normals" cluster to actually belong to the "faulty" cluster was below 3% and the probability for any "faulty" system to belong to the "normals" cluster was even lower.

The result for 3 clusters gave the following groupings:

Group 1 The "normals" and the two worst systems

15t10, 15t20, 15t20_s0, 15t30, 18t10, 18t20, 18t20_s0, 23t10, 23t20, 23t20_s0, 23t30, ***23t20_l60*** and ***23t30_l60***

Group 2 The "faulty" systems 1: lighter, cooler, smaller degree of leakage + *18t30*

18t30, 15t10_l20, 15t20_l20, 15t30_l20, 18t10_l20, 18t20_l20, 23t10_l20, 15t10_l40, 15t20_l40, 18t10_l40 and *15t10_l60*

Group 3 The "faulty" systems 2: heavier, warmer, bigger degree of leakage

18t30_l20, 23t20_l20, 23t30_l20, 15t30_l40, 18t20_l40, 18t30_l40, 23t10_l40, 23t20-_l40, 23t30_l40, 15t20_l60, 15t30_l60, 18t10_l60, 18t20_l60, 18t30_l60 and *23t10_l60*

Clustering into 4 clusters gave essentially the same result, but formed an extra cluster for the two worst systems so that group 1 contained only "normal" systems.

The figures that show all the probabilities can be found in the appendix.

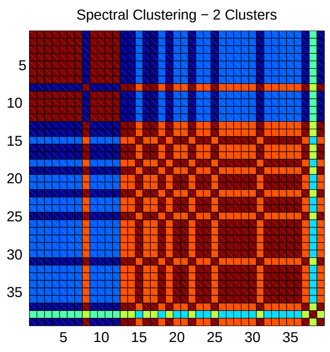

(a) 2 clusters

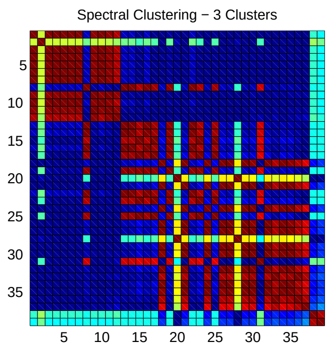

(b) 3 clusters

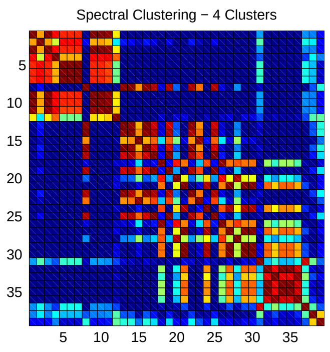

(c) 4 clusters

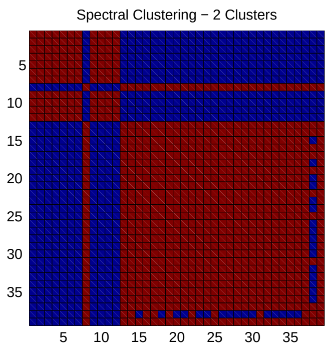

(d)

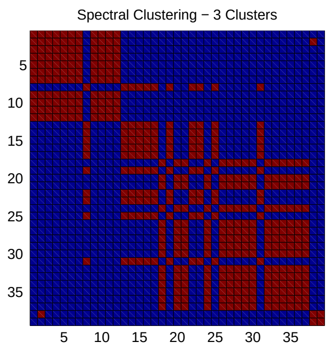

(e)

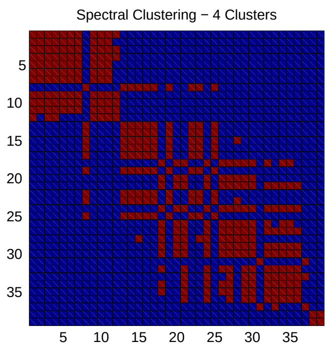

(f)

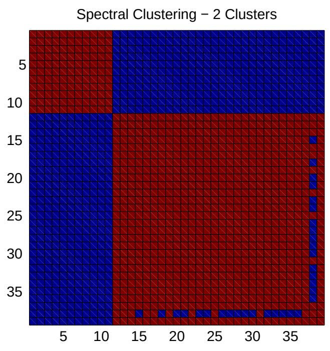

(g)

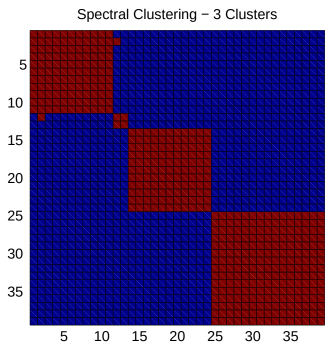

(h)

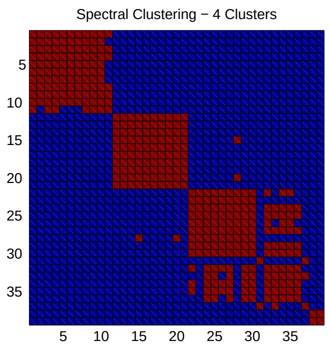

(i)

Figure 5.6: Results of spectral clustering on the PCA of the leakage data set. (a-c) show the outcome of 100 spectral clusterings into 2, 3 and 4 clusters. (d-f) show these results for the actual allocations and (g-i) show them after sorting

Discussion

The fact that system *18t30* is grouped together with the “faulty” systems is perfectly consistent with the findings of the deviation detection.

The reason that the two worst systems are grouped together with the “normals”, while the the other “faulty” systems are grouped into two clusters is most likely that they are so few and thus the optimal normalized cut separates the big group of faulty systems into two smaller ones.

5.2.1.2 Hierarchical Clustering on PCA

The hierarchical clustering algorithm described in Sec. 3.4.2 separates a given group into two clusters and is solely based on a measure of similarity like the affinity matrix.

The first group $G1$ to cluster is the whole data set.

The following systems are moved to the second cluster $G2$ in the given order: *23t30, **23t20_l60**, 23t20, 15t30, 23t20_s0, 23t10, 15t20, 15t20_s0, 18t10, 18t20, 18t20_s0, 15t10 and **23t30_s60**.*

Further splitting of $G2$ separated the two worst from the “normal” systems, while further splitting of $G1$ separated *15t10_l20, 15t10_l60* and *23t10_l60* from the other “faulty” systems. The splitting into 3 groups is visualised in Fig. 5.7.

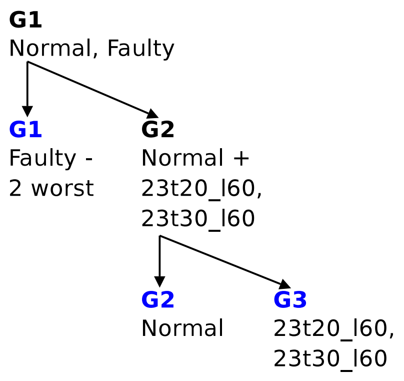

Figure 5.7: Hierarchical clustering into 3 groups

Discussion

It is interesting that the systems in group $G2$ after the first clustering are the same systems as group 1 from the spectral clustering into 3 clusters.

The clustering into the 3 groups as illustrated in Fig. 5.7 is the clearest grouping.

5.2.1.3 Clustering on KPCA

For the KPCA the approach of preserving 95% of the variance of the data was not usable, because it is not possible to reconstruct the extracted features in the input space and calculate the error.

However, as shown in Schölkopf et al. (1998), the KPCA is calculated as a kernel eigenvalue problem. These eigenvalues are sorted and divided by the sum of all eigenvalues up to the dimension of the original data. This value was then used as an estimate of the contribution of this eigenvalue. As many of the features were used so that the estimated contribution exceeded 95%.

For the systems in the leakage data set this required between 2 and 5 features, so 5 features were used. Using fewer features decreased the performance by steadily assigning the "under-described" systems to wrong groups.

The affinity matrix on the KPCA mappings is shown in Fig. 5.8 a. As before, the clustering has been tried out for 2 - 10 clusters to find usable numbers of clusters, which is shown in Fig. 5.8 b.

Spectral clustering into 2 clusters formed one cluster for the systems with 15 and 18 tons and another cluster for the systems with 23 tons. Spectral clustering into 3 clusters perfectly separated all three weight classes. More than 3 clusters did not give any useful results. Actually a fourth cluster randomly separated one of the former 3 clusters.

Hierarchical clustering was also able to perfectly separate the three weight classes. Starting with one big cluster, group 1, the weight classes 15 tons and 18 tons were moved to group 2. Further clustering of group 2 moved all systems with 15 tons to group 3.

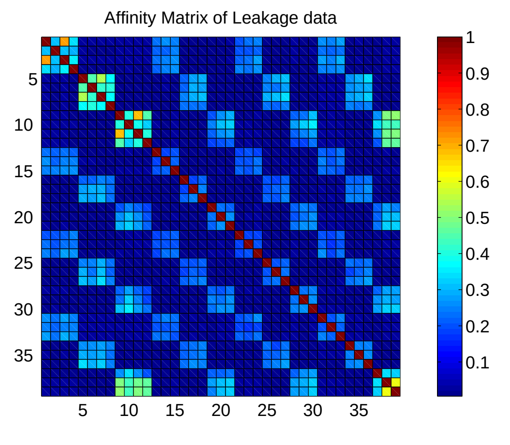

(a) Affinity Matrix on KPCA

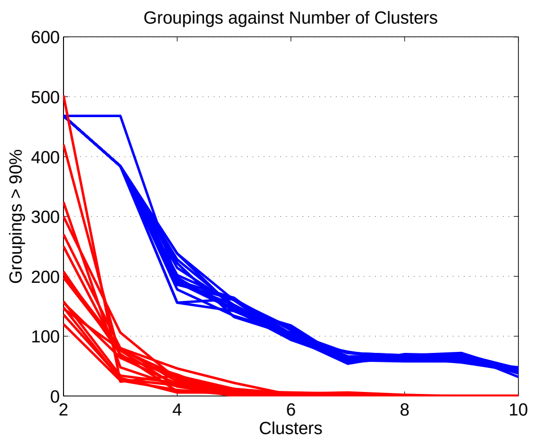

(b) Groupings against the number of clusters

Figure 5.8: (a) The affinity matrix of the Leakage data set (b) Number of systems grouped together in at least 90 out of 100 cases. Blue is for 15 spectral clusterings on the affinity matrix in (a), red is for 15 random affinity matrices

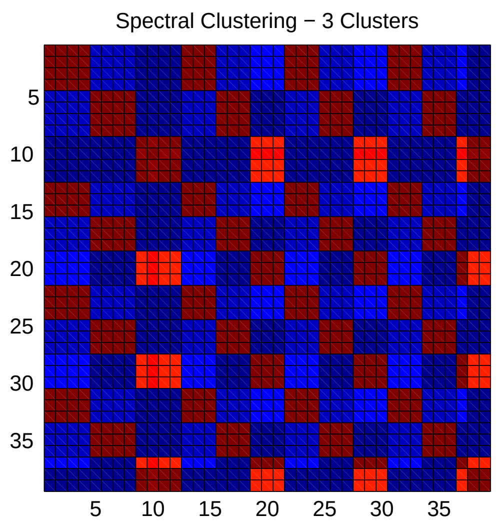

(a) Result of the spectral clustering into 3 clusters

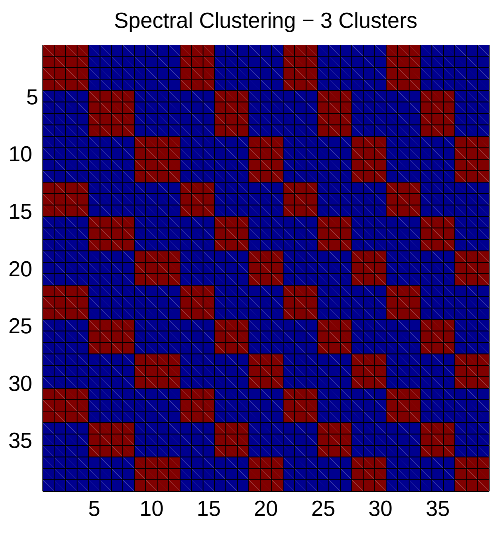

(b) Actual groupings based on the spectral clustering

Figure 5.9: Results of spectral clustering on the KPCA of the leakage data set. (a) shows the outcome of 100 spectral clusterings into 3 clusters. (b) shows these results for the actual allocations

Clustering within one of these three groups separated the systems with small and medium leakage size from those without leakage and with big leakage size. Any additional step failed to separate these groups according to the leakage size.

Discussion

Considering the affinity matrix from Fig. 5.8 a the results are not surprising. The affinity matrix already shows the three clusters very clearly.

Also it can be expected from the previous sections that the results of hierarchical clustering are comparable to those from spectral clustering.

5.2.2 Soiled Cooling System

5.2.2.1 Clustering on PCA

Spectral clustering into 2 clusters gave the following groupings:

Group 1 The "cooler" systems - lower weight, ambient temperature and soil level

15t10, 15t20, 15t20_s0, 15t30, 18t10, 18t20, 18t20_s0, 23t10, 23t20_s0, ***15t20_s15, 15t20_s30*** and ***18t20_s15***

Group 2 The "warmer" systems - higher weights, ambient temperatures and soil level

18t30, 23t20, 23t30*, 15t20_s50, 18t20_s30, 18t20_s50, 23t20_s15, 23t20-_s30* and *23t20_s50*

Spectral clustering into 3 clusters formed one group for the "cooler" systems that only contained healthy systems.

Group 1 The "cool" systems

15t10, 15t20, 15t20_s0, 15t30, 18t10, 23t10 and *23t30*

Group 2 The "medium" systems

18t20, 18t20_s0, 23t20, 23t20_s0*, 15t20_s15, 15t20_s30, 15t20_s50, 18t20-_s15, 18t20_s30* and *23t20_s15*

Group 3 The “warm” systems

> ***18t30***, *18t20_s50, 23t20_s30* and *23t20_s50*

Spectral clustering into 4 clusters gave the following groupings:

Group 1 Healthy and cool

> *15t10, 15t20, 15t20_s0, 15t30, 18t10* and *23t10*

Group 2 Mixed 1

> *18t20, 18t20_s0, 23t20_s0, 15t20_s30* and *18t20_s15*

Group 3 Mixed 2

> *23t20, 23t30, 15t20_s15, 15t20_s50, 18t20_s30* and *23t20_s15*

Group 4 Faulty and warm

> ***18t30***, *18t20_s50, 23t20_s30* and *23t20_s50*

Discussion

Clustering into two clusters separates the systems with lower weight, ambient temperature and soil degree from those with higher weight, ambient temperature and soil degree. The soiled systems in the first cluster are the ones that one would expect to be least effected by the soiled radiator, 15 tons with low and medium soil degree and 18 tons with low soil degree.

Clustering into three clusters formed one group for the “cooler” systems that only contains healthy systems and a “warm” group with only faulty systems and system *18t30*. The “medium” group contains the warmer healthy systems and the cooler faulty systems.

The clustering into four clusters gave almost the same result. The warmest system of the previous “cooler” group, *23t30*, was no longer situated in the “healthy and cool” group. The previous “medium” group was split into two mixed groups, which contain both “healthy” and “faulty” systems. The last group “faulty and warm“ was identical to the previous “warm” group.

5.2.2.2 Clustering on KPCA

As the two cooling system data sets are very similar, the results of clustering each data set are similar, too. Thus, it is not surprising that KPCA gave features that separated the soiled cooling system data into weight classes.

Alike for the cooling system with a leakage, spectral clustering into 2 clusters separated the systems with 23 tons from those with 15 and 18 tons. Clustering into 3 clusters perfectly separated all 3 weight classes. The fourth cluster separated the system *18t30* from the 18 tons cluster.

Hierarchical clustering on the other hand moved the 15 and 23 tons systems from the initial group $G1$ to the new group $G2$. Clustering this group $G2$ separated the two weight classes, but system *23t10* was grouped together with the 15 tons systems. Splitting the remaining group $G1$ separated *18t30* from the other 18 tons systems.

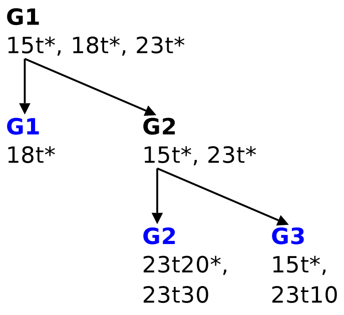

Figure 5.10: Hierarchical Clustering of the Soiled Cooling System. The * is used as a wild-card for all possible systems matching the given expression.

Discussion

The findings of this section are similar to those of clustering on KPCA of the cooling system with leakage.

5.2.3 Human Gait Data - CMU Data Set

5.2.3.1 Clustering on PCA

Spectral clustering into 2 groups created one group for the subjects 5 and 7 and another group for the subjects 6, 8 and 17. Allowing a third group separated the trials of subject 8 from subjects 6 and 17 and a fourth group split those into own groups. Clustering into 5 clusters did not give stable results.

The steps of the hierarchical clustering can be seen in 5.11.

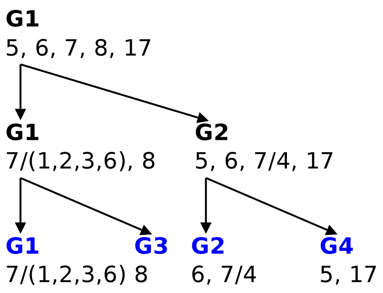

Figure 5.11: Hierarchical clustering of the CMU data set

Discussion

Although visual inspection of the trials does not show any significant differences that explain the clusters of spectral clustering, it is interesting that the different trials of the subjects 7 and 8 respectively are never split up. All these trials show “normal” walking from two individuals (cf. Tab. 4.1).

The results of hierarchical clustering are less clear in that it split up the trials of subject 7. Furthermore, 4 groups are not sufficient to delimit the limping subject 17 from all the “normal” walking styles.

5.2.3.2 Clustering on KPCA

Clustering the CMU data set based on the feature extraction with Kernel PCA did not produce any usable results.

A detailed investigation revealed that the affinities between all systems were very low. Another way of calculating the affinity between two representations might overcome this problem.

5.2.4 Human Gait Data - MIT Data Set

5.2.4.1 Clustering on PCA

Spectral clustering into 2 clusters divided the samples of walking sideways and limping from the other styles. Clustering into 3 clusters formed one cluster for normal walking, one for walking sideways and another one of waddling, swaying, jogging and limping. Clustering into 4 or more clusters did not result in reasonable separations.

Hierarchical clustering found the clusters shown in Fig. 5.12

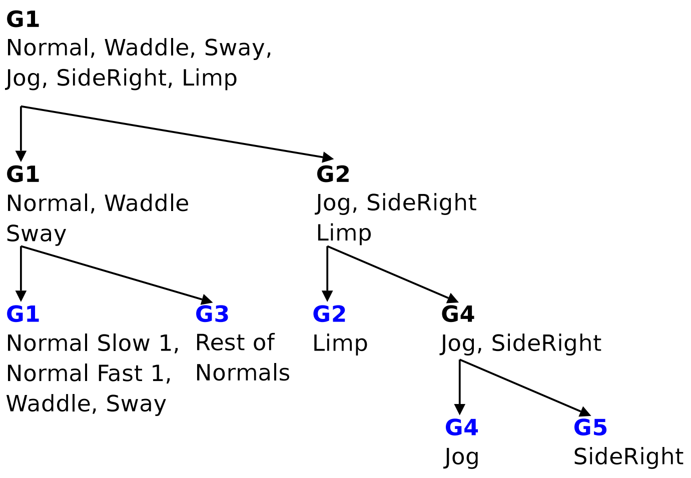

Figure 5.12: Hierarchical clustering of the MIT data set

Discussion

The groupings found on this data set can be easily explained by the assumption that from all the walking styles, walking sideways is the most odd one, followed by jogging and limping. Although not perfectly normal, but still following the same motion pattern, swaying and waddling are closest to the samples of normal walking. This is also consistent with the findings of the deviation detection on this data set.

6 Summary and Conclusion

The proposed approach provides the ability to efficiently describe large amounts of data with a compressed representation, compare such compressed representations and finally detect deviations among groups of systems based on these compressed representations.

The compressed representation is needed to

- reduce the amount of data to transfer.
  This allows transmission of data over low bandwidth media such as radio communication, which is important in environments with many mechatronical systems.
- reduce requirements of storage space and processing time and facilitates handling of large amounts of systems.
  Hence the scalability of the proposed approach is significantly improved.

The second step, comparing compressed representations, computes measures of similarity between systems and combines them in a so-called affinity matrix. The successive computations are exclusively based on this measure. Consequently, this step decouples the representation from the deviation detection. As a result, additional representation methods can be added without the need to adapt the deviation detection methods as well as vice versa.

In the proposed approach, the final deviation detection is done in two different ways:

- the probability for each system to be observed given all the other systems is calculated. Systems with a probability below a certain threshold, e.g. 5%, are flagged as deviating.

- all systems are clustered. Systems with similar features are hereby clustered together. In a population where most of the systems are “healthy” (such that they appear to be similar using a certain representation) the deviating systems form one or more smaller clusters.

These two methods can also be combined. For example, the clustering can be done using one compressed representation and subsequently the probabilities for each system to be “normal” within a cluster can be calculated using another representation. It might have been a very successful approach for the soiled cooling system data set to first cluster it using KPCA and then calculate the probabilities based on PCA, but was omitted due to the size of the data set.

Using the proposed approach to analyze four data sets from two different domains, a simulated cooling system and human gait data, demonstrates it applicability to simulated data with systems from well separated classes as well as real world data.

In contrast to the method from Byttner et al. (2008), the proposed approach is not only able to detect vehicles with a leakage level of 60%, but any vehicle with a leakage. Furthermore, our approach is not limited to finding deviations within a set of systems, but is also able to group this set into subsets with similar properties.

However, there is much room for further improvements.

The method to determine the number of kernel principal components that should be used to calculate the affinity matrix lacks a mathematical justification.

Also, the other methods to compare subspaces, overlapping volume and reconstruction error with interchanged subspaces, should be tried out.

Besides, the feature extraction methods need to be extended to online versions and the applicability of the method on a bigger real word data needs to be analyzed.

Bibliography

[Aickelin et al. 2004] U. Aickelin, J. Greensmith, and J. Twycross: Immune System Approaches to Intrusion Detection – A Review. In: *Proceedings of Artificial Immune Systems: Third International Conference, ICARIS 2004*, Springer, 2004

[Byttner et al. 2008] S. Byttner, M. Svensson, and T. Rognvaldsson: *Self-organized modeling for vehicle fleet based fault detection.* Submitted to SAE International. 2008

[Efron 1979] B. Efron: Bootstrap Methods: Another Look at the Jackknife. In: *The Annals of Statistics* 7(1):1–26, 1979

[Hastie et al. 2001] T. Hastie, R. Tibshirani, and J. Friedman: *The Elements of Statistical Learning: Data Mining, Inference, and Prediction.* Springer, New York, 2001

[Hinton and Salakhutdinov 2006] G. Hinton and R. Salakhutdinov: Reducing the Dimensionality of Data with Neural Networks. In: *SCIENCE* 313:504–507, 2006

[Hodge and Austin 2004] V. J. Hodge and J. Austin: A Survey of Outlier Detection Methodologies. In: *Artificial Intelligence Review* 22:85–126, 2004

[Hsu et al. 2005] E. Hsu, K. Pulli, and J. Popović: Style translation for human motion. In: *Proceedings of ACM SIGGRAPH 2005* 24(3):1082–1089, 2005

[Huang et al. 2006a] L. Huang, X. Nguyen, M. Garofalakis, M. Jordan, A. Joseph, and N. Taft: In-network PCA and anomaly detection / UC Berkeley Tech. Rep. Aug. 2006

[Huang et al. 2006b] L. Huang, X. Nguyen, M. Garofalakis, M. Jordan, A. Joseph, and N. Taft: *Distributed PCA and network anomaly detection.* Submitted to NIPS. 2006

[Krzanowski 1979] W. J. Krzanowski: Between-Groups Comparison of Principal Components. In: *Journal of the American Statistical Association* 74(367):703–707, 1979

[Lakhina et al. 2004] A. Lakhina, M. Crovella, and C. Diot: Diagnosing network-wide traffic anomalies. In: *SIGCOMM Computer Communication Review* 34(4):219–230, 2004

[Macnaughton-Smith et al. 1964] P. Macnaughton-Smith, W. Williams, M. Dale, and L. Mockett: Dissimilarity analysis: A new technique of hierarchical sub-division. In: *Nature* 202:1034–1035, 1964

[Markou and Singh 2003a] M. Markou and S. Singh: Novelty detection: a review—part 1: statistical approaches. In: *Signal Processing* 83(12):2481–2497, 2003

[Markou and Singh 2003b] M. Markou and S. Singh: Novelty detection: a review—part 2: neural network based approaches. In: *Signal Processing* 83(12):2499–2521, 2003

[Oja 1982] E. Oja: Simplified neuron model as a principal component analyzer. In: *Journal of Mathematical Biology* 15(3):267–273, 1982

[Schölkopf et al. 1998] B. Schölkopf, A. Smola, and K.-R. Müller: Nonlinear Component Analysis as a Kernel Eigenvalue Problem. In: *Neural Computation* 10(5):1299–1319, 1998

[Shi and Malik 2000] J. Shi and J. Malik: Normalized cuts and image segmentation. In: *IEEE Transactions on Pattern Analysis and Machine Intelligence* 22(8):888–905, 2000

[Sun and Cheng 2006] X. Sun and Q. Cheng: On Subspace Distance. In: *Lecture Notes in Computer Science* 4142:81–89, 2006

[Vachkov 2006] G. Vachkov: Intelligent Data Analysis for Performance Evaluation and Fault Diagnosis in Complex Systems. In: *2006 IEEE International Conference on Fuzzy Systems*, 2006

[Wang et al. 2006] L. Wang, X. Wang, and J. Feng: Subspace distance analysis with application to adaptive Bayesian algorithm for face recognition. In: *Pattern Recognition* 39(3):456–464, 2006

Appendix

A.1 Cooling System with a Leakage: Spectral Clustering on PCA

The following figures show the probabilities for the systems of a group GX to belong to GY

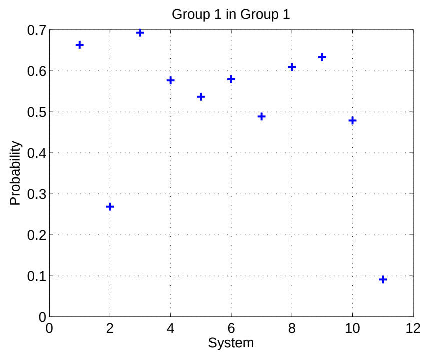

G1 in G1

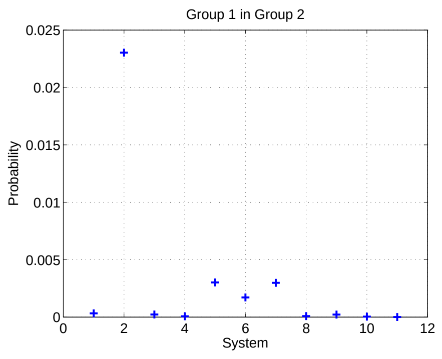

G1 in G2

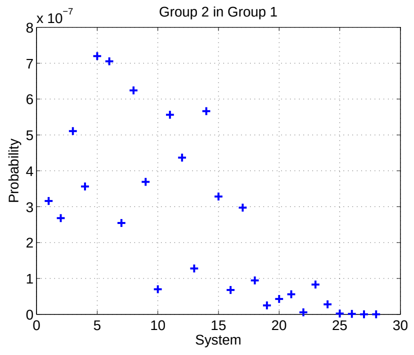

G2 in G1

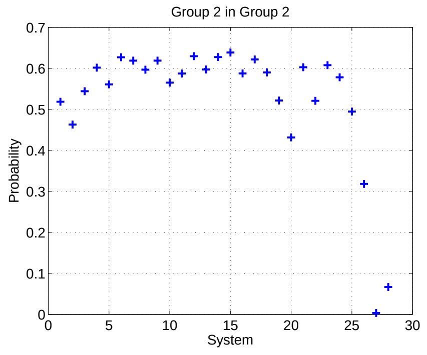

G2 in G2

Figure A.1: Grouping probabilities for 2 groups

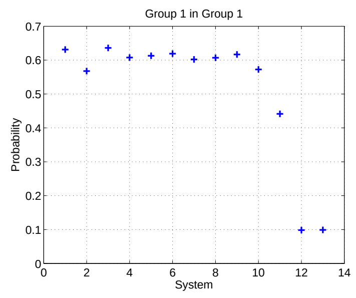

G1 in G1

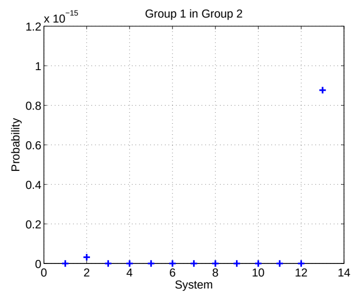

G1 in G2

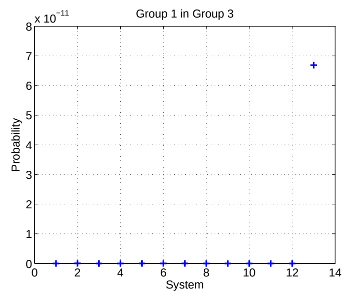

G1 in G3

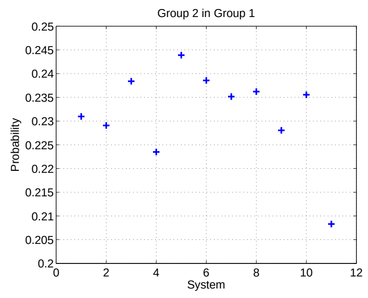

G2 in G1

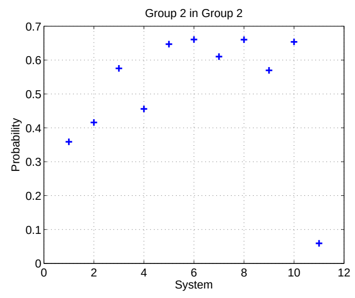

G2 in G2

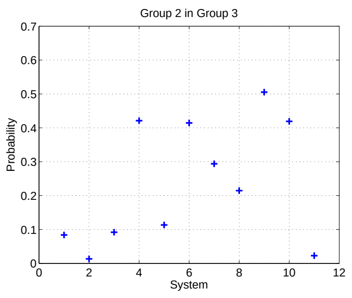

G2 in G3

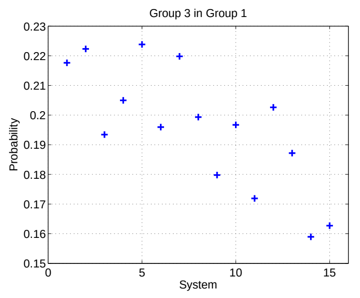

G3 in G1

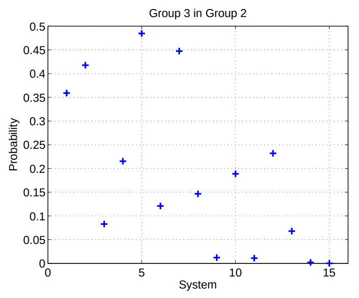

G3 in G2

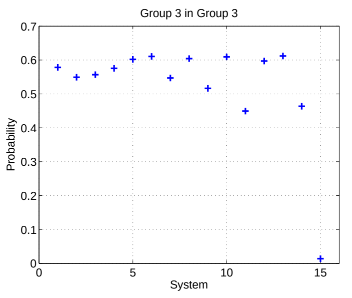

G3 in G3

Figure A.2: Grouping probabilities for 3 groups

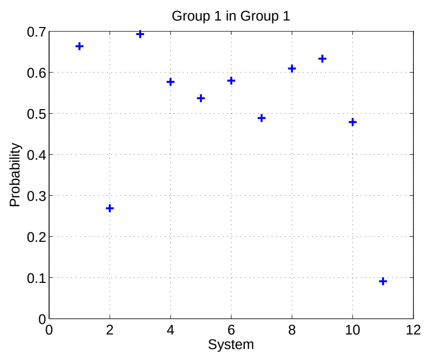

G1 in G1

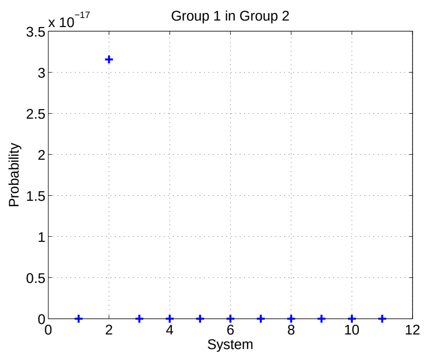

G1 in G2

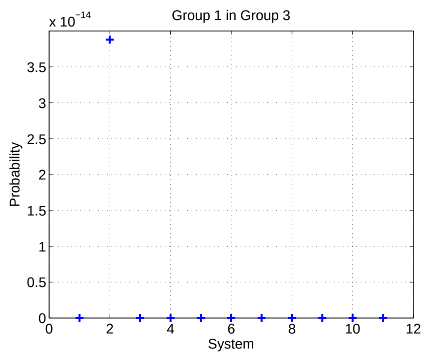

G1 in G3

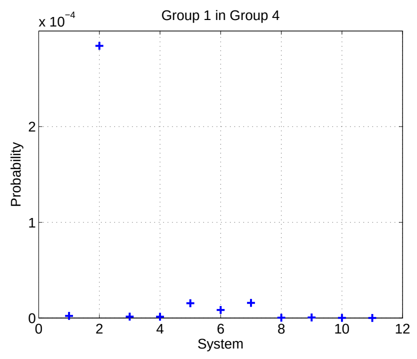

G1 in G4

Figure A.3: Grouping probabilities for 4 groups: Group 1

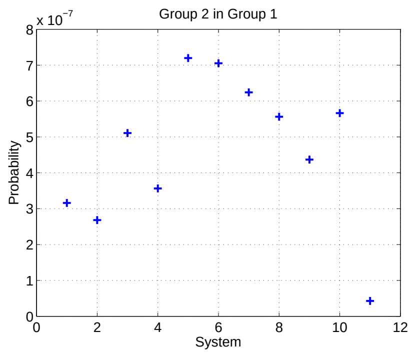

G2 in G1

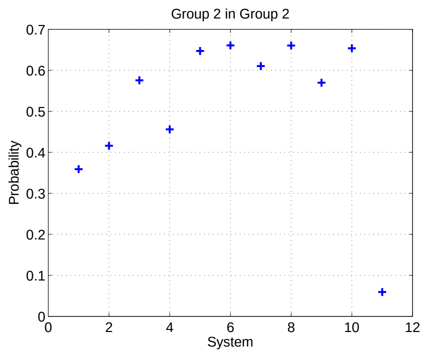

G2 in G2

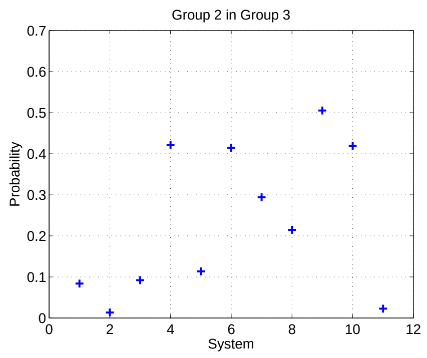

G2 in G3

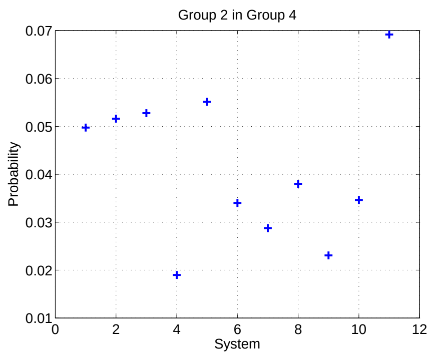

G2 in G4

Figure A.4: Grouping probabilities for 4 groups: Group 2

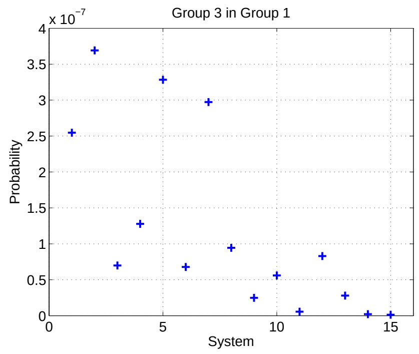

G3 in G1

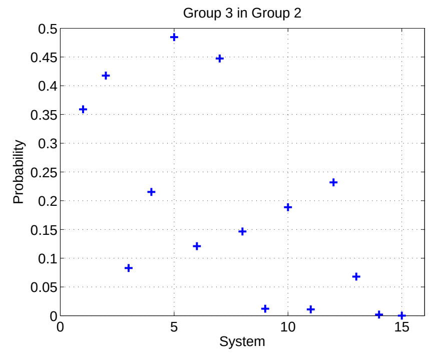

G3 in G2

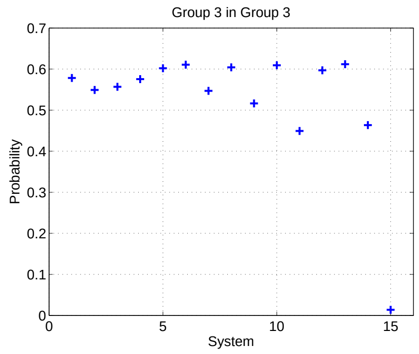

G3 in G3

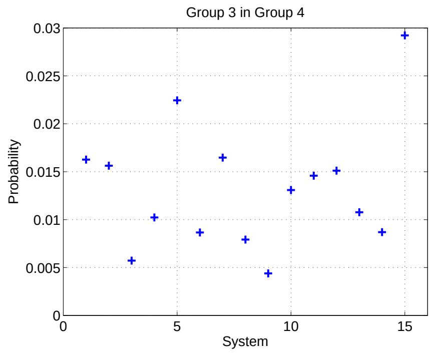

G3 in G4

Figure A.5: Grouping probabilities for 4 groups: Group 3

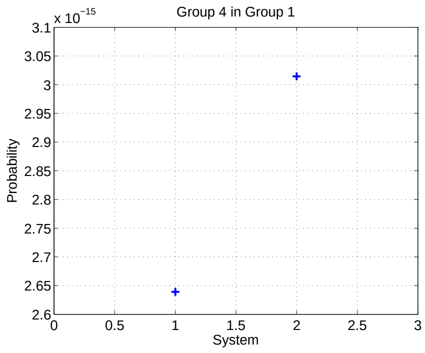

G4 in G1

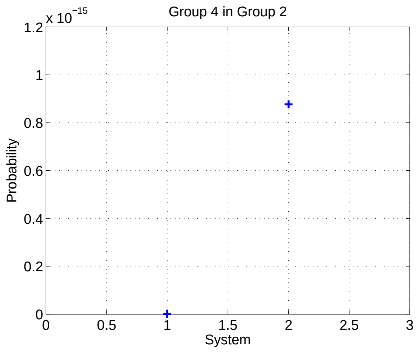

G4 in G2

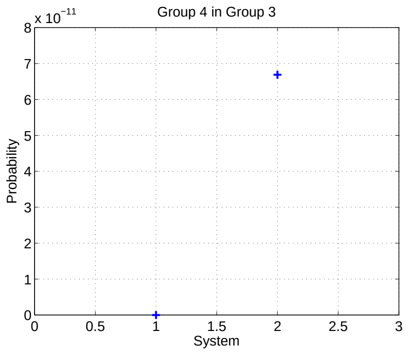

G4 in G3

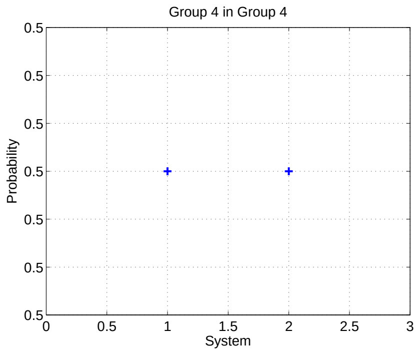

G4 in G4

Figure A.6: Grouping probabilities for 4 groups: Group 4